

PREPARED FOR SUBMISSION TO JINST

INTERNATIONAL CONFERENCE ON FUSION REACTOR DIAGNOSTICS - ICFRD2021

SEPTEMBER 6-10, 2021

VARENNA, ITALY

First equilibrium reconstruction for ITER with the code NICE

B. Faugas,¹ J. Blum, C. Boulbe

Université Côte d'Azur, CNRS, Inria, LJAD, Parc Valrose, 06108 Nice Cedex 2, France

E-mail: blaise.faugeras@univ-cotedazur.fr

ABSTRACT: In this short paper we present the first application of the IMAS compatible code NICE to equilibrium reconstruction for ITER geometry. The inverse problem is formulated as a least square problem and the numerical methods implemented in NICE in order to solve it are presented. The results of a numerical experiment are shown: a reference equilibrium is computed from which a set of synthetic magnetic measurements are extracted. Then these measurements are used successfully to reconstruct the equilibrium of the plasma.

KEYWORDS: Simulation methods and programs, Nuclear instruments and methods for hot plasma diagnostics

¹Corresponding author.

Contents

1	Introduction	1
2	Inverse problem formulation	1
2.1	Free-boundary plasma equilibrium	1
2.2	The inverse reconstruction problem	4
3	Numerical methods	5
3.1	Discretization of the direct model	5
3.2	The discrete identification problem	5
4	Numerical experiment	7
5	Conclusion	9

1 Introduction

Numerical reconstruction of the plasma equilibrium in a tokamak is an important and long standing subject in fusion plasma science [2, 24, 27, 34, 37, 39]. The resolution of this inverse problem consists in the computation of the poloidal flux function and of the plasma boundary as well as the identification of two non-linear source term functions known as p' and ff' in the Grad-Shafranov equation [18, 26, 35]. It is needed on the one hand for a posteriori analysis of experimental equilibrium configurations and on the other hand for real time control of the plasma during a discharge. The basic set of measurements needed and used are magnetic probes and flux loops which provide values of the poloidal magnetic field and flux at several points surrounding the vacuum vessel and the plasma. All free boundary reconstruction codes (e.g. [3, 4, 6, 9, 10, 25, 28, 30, 40]) primarily use these magnetic measurements which proved to be sufficient to identify correctly the plasma boundary and the averaged plasma current density profile [4]. The goal of this paper is to present a first test of the adaptation of the numerical tools developed by the authors, namely the code NICE [9], to the foreseen ITER configuration. NICE stands for "Newton direct and Inverse Computation for Equilibrium".

Next Section 2 is devoted to the formulation of the direct model and the inverse problem. In Section 3 we discuss the numerical methods which we have developed for their resolution and finally in Section 4 a first test numerical experiment is presented for ITER configuration.

2 Inverse problem formulation

2.1 Free-boundary plasma equilibrium

The equations which govern the equilibrium of a plasma in the presence of a magnetic field in a tokamak are on the one hand Maxwell's equations satisfied in the whole of space (including the

plasma):

$$\nabla \cdot \mathbf{B} = 0, \quad \nabla \times \left(\frac{\mathbf{B}}{\mu} \right) = \mathbf{j}, \quad (2.1)$$

and on the other hand the equilibrium equation for the plasma itself

$$\nabla p = \mathbf{j} \times \mathbf{B}, \quad (2.2)$$

where \mathbf{B} is the magnetic field, μ is the magnetic permeability, p is the kinetic pressure and \mathbf{j} is the current density. We refer to standard text books (e.g. [2, 15, 17, 23, 38]) and to [20] for details of the derivation and only state the needed equations in what follows which is a summary of what can be found in [9].

Introducing a cylindrical coordinate system $(\mathbf{e}_r, \mathbf{e}_\phi, \mathbf{e}_z)$ ($r = 0$ is the major axis of the tokamak torus) and assuming axial symmetry equations (2.1) and (2.2) reduce to the following equation for the magnetic poloidal flux $\psi(r, z)$ in the poloidal plane $\Omega_\infty = (0, \infty) \times (-\infty, \infty)$:

$$-\Delta^* \psi = j_\phi, \quad (2.3)$$

where j_ϕ is the toroidal component of \mathbf{j} , and the second order elliptic differential operator Δ^* is defined by

$$\Delta^* \psi := \partial_r \left(\frac{1}{\mu_0 r} \partial_r \psi \right) + \partial_z \left(\frac{1}{\mu_0 r} \partial_z \psi \right) := \nabla \cdot \left(\frac{1}{\mu_0 r} \nabla \psi \right). \quad (2.4)$$

Here ∇ is the 2D operator in the (r, z) -plane and μ_0 is the magnetic permeability of vacuum (in this work we consider only air-transformer tokamaks such as ITER).

The magnetic field can be decomposed in poloidal and toroidal components

$$\mathbf{B} = \mathbf{B}_p + \mathbf{B}_\phi, \quad \mathbf{B}_p = \frac{1}{r} [\nabla \psi \times \mathbf{e}_\phi], \quad \mathbf{B}_\phi = B_\phi \mathbf{e}_\phi = \frac{f}{r} \mathbf{e}_\phi, \quad (2.5)$$

where f is the diamagnetic function. Equation (2.5) shows that the magnetic surfaces are generated by the rotation of the iso-flux lines around the axis of the torus.

The toroidal component of the current density j_ϕ is zero everywhere outside the plasma domain and the poloidal field coils (and possibly the passive structures). The different sub-domains of the poloidal plane of a schematic tokamak (see Fig. 1) as well as the corresponding expression for j_ϕ are described below:

- Ω_L is the domain accessible to the plasma. Its boundary is the limiter $\partial\Omega_L$.
- Ω_p is the plasma domain where equations (2.2) and (2.1) imply that p and f are constant on each magnetic surface i.e. $p = p(\psi)$ and $f = f(\psi)$. One then deduces the so-called Grad-Shafranov equilibrium equation in the plasma [18, 26, 35]

$$-\Delta^* \psi = r p'(\psi) + \frac{1}{\mu_0 r} (f f')(\psi). \quad (2.6)$$

The right-hand side of (2.6) is the toroidal component j_ϕ of the current density in the plasma. The plasma domain is unknown, i.e. $\Omega_p = \Omega_p(\psi)$, and this is a free boundary problem. This domain is defined by its boundary which is the outermost closed ψ iso-contour contained

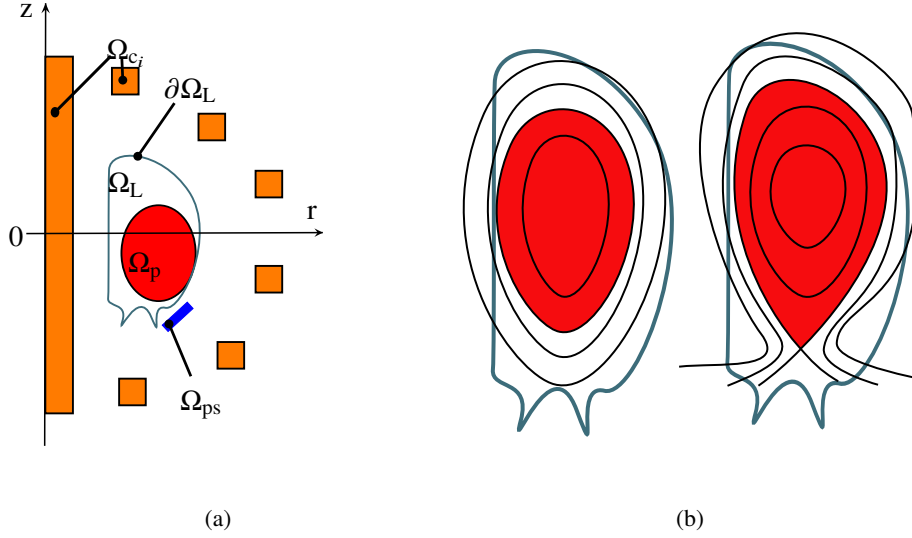


Figure 1: Left (a): schematic representation of the poloidal plane of a tokamak. Ω_p is the plasma domain, Ω_L is the limiter domain accessible to the plasma, Ω_{c_i} represent poloidal field coils and the central solenoid (corresponding to the IMAS pf_active IDS), Ω_{ps} the passive structures. Right (b): example of a plasma whose boundary is defined by the contact with limiter (left) or by the presence of an X-point (right).

within the limiter Ω_L . The plasma can either be limited if this iso-contour is tangent to the limiter $\partial\Omega_L$ or defined by the presence of an X-point (see Fig. 1). Functions p' and ff' are zero outside Ω_p .

The current density is non-linear in ψ due to the non-linear functions p' and ff' and the definition of the plasma domain $\Omega_p(\psi)$. While $\Omega_p(\psi)$ is fully determined for a given ψ , the two functions p' and ff' are not determined in this modelization. It is the goal of the inverse equilibrium reconstruction problem to determine them. For now let us consider that we are given two functions $\mathcal{A}(\psi_N)$ and $\mathcal{B}(\psi_N)$ such that

$$j_\phi = \lambda \left(\frac{r}{r_0} \mathcal{A}(\psi_N) + \frac{r_0}{r} \mathcal{B}(\psi_N) \right). \quad (2.7)$$

Here r_0 is the major radius of the tokamak vacuum chamber and λ is a scaling coefficient. The normalized poloidal flux $\psi_N(r, z)$ is

$$\psi_N(r, z) = \frac{\psi(r, z) - \psi_a(\psi)}{\psi_b(\psi) - \psi_a(\psi)}. \quad (2.8)$$

with ψ_a and ψ_b being the flux values at the magnetic axis and at the boundary of the plasma.

- Each domain Ω_{c_i} , $i = 1, \dots, N_C$ represent one of the N_C coils carrying currents that is to say poloidal field coils as well as the central solenoid (this corresponds to the IMAS pf_active IDS). The expression of the current density in the i -th coil is

$$j_\phi = \frac{I_i}{S_i}, \quad (2.9)$$

where S_i is the section area of the coil and I_i is a given measured current.

- Ω_{ps} represents passive structures where the induced current density is assumed to be 0 in this work but can be considered to be measured and given in the same form as Eq. (2.9)

To sum up, given functions \mathcal{A} and \mathcal{B} , and currents $\mathbf{I} = \{I_i\}_{i=1}^{N_C}$ in the coils, the free-boundary equilibrium equation for $\psi(r, z)$ on Ω_∞ is the following non-linear boundary value problem

$$\begin{cases} -\Delta^* \psi = \begin{cases} \lambda \left(\frac{r}{r_0} \mathcal{A}(\psi_N) + \frac{r_0}{r} \mathcal{B}(\psi_N) \right) & \text{in } \Omega_p(\psi), \\ \frac{I_i}{S_i} & \text{in } \Omega_{c_i}, \\ 0 & \text{elsewhere,} \end{cases} \\ \psi(0, z, t) = 0, \\ \lim_{\|(r, z)\| \rightarrow +\infty} \psi(r, z) = 0. \end{cases} \quad (2.10)$$

This formulation on an infinite domain is not used directly in computations where we use finite elements on a truncated bounded domain. The infinite domain is reduced to a semi circular computational domain by an uncoupling procedure [1, 16]. We chose a semi-circle Γ of radius ρ_Γ surrounding the coil domains Ω_{c_i} and define the computation domain Ω having boundary $\partial\Omega = \Gamma \cup \Gamma_0$, where $\Gamma_0 = \{(0, z), z \in [-\rho_\Gamma, \rho_\Gamma]\}$.

The weak formulation of the equilibrium problem on which the finite element method relies uses a function space V defined in [20] and can be written as:

Given function \mathcal{A} and \mathcal{B} , and currents \mathbf{I} , find $\psi \in V$ such that for all $\xi \in V$

$$\mathbf{a}(\psi, \xi) + \mathbf{c}(\psi, \xi) - \mathbf{J}_p(\psi, \xi; \mathcal{A}, \mathcal{B}) - \ell(\mathbf{I}, \xi) = 0, \quad (2.11)$$

where

$$\begin{aligned} \mathbf{a}(\psi, \xi) &:= \int_{\Omega} \frac{1}{\mu_0 r} \nabla \psi \cdot \nabla \xi \, dr dz, \\ \mathbf{J}_p(\psi, \xi; \mathcal{A}, \mathcal{B}) &:= \int_{\Omega_p(\psi)} \lambda \left(\frac{r}{r_0} \mathcal{A}(\psi_N) + \frac{r_0}{r} \mathcal{B}(\psi_N) \right) \xi \, dr dz, \\ \ell(\mathbf{I}, \xi) &:= \sum_{i=1}^{N_C} \frac{I_i}{S_i} \int_{\Omega_{c_i}} \xi \, dr dz, \end{aligned} \quad (2.12)$$

and the bilinear form $\mathbf{c} : V \times V \rightarrow \mathbb{R}$ is accounting for the boundary conditions at infinity. We refer to [20] for its precise expression and to [19, Chapter 2.4] for the details on its the derivation. Alternative approaches for the incorporation of boundary conditions at infinity were more recently presented in [12].

2.2 The inverse reconstruction problem

Magnetics constitute the basic set of experimental measurements used in equilibrium reconstruction for the identification of functions \mathcal{A} and \mathcal{B} . They consist in measurements of projections of the poloidal magnetic field, $\mathbf{B}_p \cdot \mathbf{d}$ at several locations around the vacuum vessel of the tokamak (the unit vector \mathbf{d} varies with each B-probe) and of flux loops measurements, noted $F(\psi)$, at several locations too.

At this point we have defined a direct model given by the equilibrium equation (2.11), control variables \mathcal{A} and \mathcal{B} , and measurements to which are attached experimental errors represented by the standard deviations σ s in Eq. (2.14) below. The identification problem can now be formulated as a constrained minimization problem for the following cost function:

$$J(\psi, \mathcal{A}, \mathcal{B}) := J_{obs}(\psi) + R(\mathcal{A}) + R(\mathcal{B}), \quad (2.13)$$

where the least-square misfit term is

$$J_{obs}(\psi) := \sum_{i=1}^{N_B} \frac{1}{2\sigma_{Bi}^2} ((\mathbf{B}_p(r_i, z_i) \cdot \mathbf{d}_i) - B_{p,obs}^i)^2 + \sum_{i=1}^{N_F} \frac{1}{2\sigma_{Fi}^2} (F(\psi)_i - F_{obs}^i)^2 \quad (2.14)$$

and the regularization term $R(\mathcal{A})$ is defined as

$$R(\mathcal{A}) := \frac{\varepsilon_{\mathcal{A}}}{2} \int_0^1 (\mathcal{A}''(x))^2 dx + \frac{\alpha_{\mathcal{A}}}{2} |\mathcal{A}(1)|^2. \quad (2.15)$$

The $R(\mathcal{B})$ term is defined similarly. Parameters ε enable to tune the smoothness of the identified functions whereas parameters α tune the penalization to zero of their value on the plasma boundary. The inverse problem consists in the minimization of J (2.13) under the constraint of the model equation (2.11).

3 Numerical methods

3.1 Discretization of the direct model

Equilibrium equation (2.11) is discretized using a P1 finite element method based on a triangular mesh. From now on let us also assume that functions \mathcal{A} and \mathcal{B} are decomposed in a basis of functions ϕ_i defined on $[0, 1]$. We use cubic spline functions in this work and

$$\mathcal{A}(x) = \sum_{i=1}^{N_{\mathcal{A}}} u_{\mathcal{A}i} \phi_i(x), \quad \mathcal{B}(x) = \sum_{i=1}^{N_{\mathcal{B}}} u_{\mathcal{B}i} \phi_i(x). \quad (3.1)$$

Let us denote $\mathbf{u} = (\mathbf{u}_{\mathcal{A}}, \mathbf{u}_{\mathcal{B}})$ of size N_u the vector of degrees of freedom of \mathcal{A} and \mathcal{B} in the decomposition basis. Classically approximating ψ by $\psi_h = \sum_{i=1}^N \psi_i \lambda_i(r, z)$ on the finite element approximation space as well as the operators of (2.11) and taking all basis elements λ_i as test functions leads to the following non-linear system of N equations:

$$(\mathbf{A} + \mathbf{C})\boldsymbol{\psi} - \mathbf{J}_p(\boldsymbol{\psi}, \mathbf{u}) - \mathbf{L}\mathbf{I} = 0 \quad (3.2)$$

where $\boldsymbol{\psi}$ denotes the vector of finite element coefficients $\{\psi_i\}_{i=1}^N$ and other notations are obvious.

3.2 The discrete identification problem

Using the discrete variables of the preceding section, cost function (2.13) can also be discretized leading to the following expression

$$J(\boldsymbol{\psi}, \mathbf{u}) := \frac{1}{2} \|\mathbf{H}\boldsymbol{\psi} - \mathbf{m}\|^2 + \frac{1}{2} \|\mathbf{R}\mathbf{u}\|^2. \quad (3.3)$$

In order to lighten notations the $\frac{1}{\sigma}$ terms have been dropped and are assumed to be included in the observation operator \mathbf{H} and in the measurements \mathbf{m} . The last term involving matrice \mathbf{R} is the discretization of the regularization terms in which we have gathered the contributions from functions \mathcal{A} and \mathcal{B} .

The discrete identification problem can now be stated as

$$\min_{\psi, \mathbf{u}} J(\psi, \mathbf{u}) \quad (3.4)$$

subject to the constraint of the non-linear model

$$(\mathbf{A} + \mathbf{C})\psi - \mathbf{J}_p(\psi, \mathbf{u}) - \mathbf{L}\mathbf{I} = 0 \quad (3.5)$$

This problem is solved thanks to a quasi-SQP algorithm with reduced Hessian (QSQP). SQP methods are well documented [21, 31] and for fusion application we refer to [5, Appendix A] and [9, 11]. An SQP method can be seen as a Newton method to solve the non-linear system given by the first order optimality condition for the Lagrangian of the PDE-constrained optimization problem.

The QSQP method we use is the following 2 steps iterative algorithm:

1. control variable update step

$$\mathbf{M}(\mathbf{u}^{n+1} - \mathbf{u}^n) = -\mathbf{h} \quad (3.6)$$

2. state variable update step

$$\psi^{n+1} = \psi^n + \delta\psi + \mathbf{S}(\mathbf{u}^{n+1} - \mathbf{u}^n) \quad (3.7)$$

where

$$\delta\psi = -[(\mathbf{A} + \mathbf{C})\psi^n - D_\psi \mathbf{J}_p(\psi^n, \mathbf{u}^n)]^{-1}[(\mathbf{A} + \mathbf{C})\psi^n - \mathbf{J}_p(\psi^n, \mathbf{u}^n) - \mathbf{L}\mathbf{I}], \quad (3.8)$$

$$\mathbf{S} = -[(\mathbf{A} + \mathbf{C})\psi^n - D_\psi \mathbf{J}_p(\psi^n, \mathbf{u}^n)]^{-1}[-D_{\mathbf{u}} \mathbf{J}_p(\psi^n, \mathbf{u}^n)], \quad (3.9)$$

$$\mathbf{M} = \mathbf{R}^T \mathbf{R} + \mathbf{S}^T \mathbf{H}^T \mathbf{H} \mathbf{S} \quad (3.10)$$

and

$$\mathbf{h} = \mathbf{R}^T \mathbf{R} \mathbf{u}^n + \mathbf{S}^T \mathbf{H}^T (\mathbf{H} \psi^n - \mathbf{m}) + \mathbf{S}^T \mathbf{H}^T \mathbf{H} \delta\psi \quad (3.11)$$

At each iteration this algorithm demands the resolution of $N_u + 1$ linear systems (3.8)-(3.9) of size N involving the same matrix with different right-hand sides which can be done very efficiently and of one smaller linear system of size N_u in (3.6).

The performance of the QSQP method used for the resolution of the identification problem relies on the accuracy of the derivative terms $D_\psi \mathbf{J}_p$, $D_{\mathbf{u}} \mathbf{J}_p$. In this work we have implemented the exact derivatives of the fully discretized operators. This essential but very technical work is not further detailed here and we refer to [20, section 3.2 and 3.3] for details.

4 Numerical experiment

The numerical methods presented in the previous sections are implemented in the code NICE [9] with which the following numerical experiment is conducted. ITER machine description providing the points defining the limiter contour, the poloidal field coils and a description of the magnetic sensors (196 poloidal magnetic field probes and 22 differential flux loops) are read from the *wall*, *pf_active* and *magnetics* Interface Data Structure (IDS) from the ITER Integrated Modelling and Analysis Suite (IMAS) [22]. From this machine description NICE builds the triangular mesh used with the finite elements computations.

We generate a reference equilibrium by solving the so-called inverse static equilibrium problem [9, 20] that is to say finding the currents in the coils giving a desired prescribed plasma boundary. For this reference computation the unknown function are given analytically as $\mathcal{A}(x) = (1 - x^{1.5})^{0.9}$ and $\mathcal{B}(x) = (1 - x^{0.9})^{1.5}$. The scaling factor λ in the current density (2.7) is computed such that the total plasma current is $I_p = 12$ [MA]. The vacuum toroidal field is $B_0 = 5.3$ [T] and $r_0 = 6.2$ [m]. Synthetic magnetic measurements are computed from this reference equilibrium.

Then in a second step these measurements are plugged in cost function (3.3) and the optimization problem is solved using the iterative QSQP algorithm presented above. The initial guess for this resolution consists in a given circular plasma domain in which the flux ψ is a constant and outside of which it is 0, as well as affine functions $\mathcal{A}(x) = \mathcal{B}(x) = 1 - x$. Convergence is assumed when the relative residue for the vector of unknowns $\mathbf{X} = (\boldsymbol{\psi}, \mathbf{u})$ satisfies $\|\mathbf{X}^{k+1} - \mathbf{X}^k\|/\|\mathbf{X}^k\| < 10^{-12}$.

The finite element mesh is composed of $N = 11856$ nodes among which 11772 correspond to free values of ψ (the remaining correspond to the imposed boundary condition $\psi = 0$ on the axis $r = 0$). Each function to be identified is decomposed in 11 cubic splines defined on $[0, 1]$ with knots at $0, 0.1, \dots, 1$. Therefore \mathbf{X} is a vector of size $11772 + 2 \times 11 = 11794$.

The regularization parameters ε are tuned to their lowest value, typically 10^{-2} , avoiding oscillations in the reconstructed profiles or non convergence of the code. The penalization parameters are set to $\alpha = 10^{12}$.

Starting from the initial guess described above, which is far from the reference solution we want to recover, the algorithm needs 16 iterations to converge to a relative residue of 4×10^{-14} . In this test configuration one iteration takes about 800 ms on a laptop with an Intel CPU at 2.90 GHz. This computation time is highly dependent on the mesh size and is limited by the performance of the linear solver. The reconstructed flux map is shown on Figure 2. The plasma boundary is perfectly recovered. The fit to measurements is excellent with a root mean square error of 10^{-4} on magnetic probes and flux loops.

Figure 3 shows the reference and identified p' and ff' profiles. A typical feature of the equilibrium reconstruction inverse problem using only magnetic measurements appears: the computed error bars on the reconstructed profiles increase when approaching the magnetic axis. However even if the p' and ff' profiles are not perfectly identified for low ψ_N values, the flux surface averaged current density profile $j_{tor} = \langle j_\phi/r \rangle < 1/r \rangle$ and the safety factor q are very well recovered.

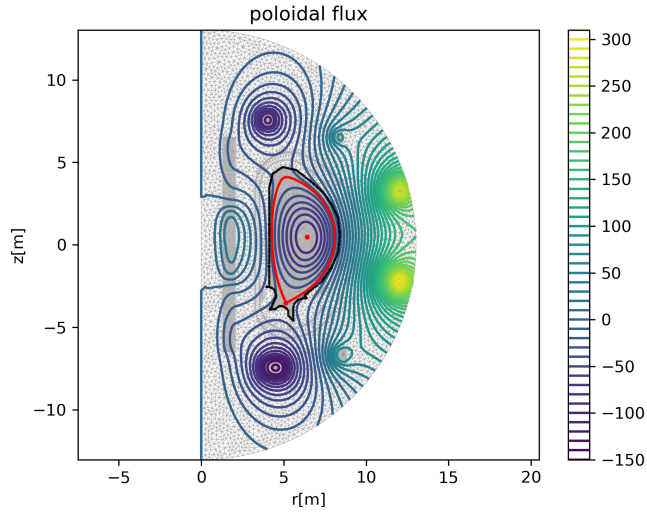


Figure 2: Reconstructed poloidal flux map (ψ in [Wb]). The plasma boundary with an X-point and the magnetic axis are shown in red.

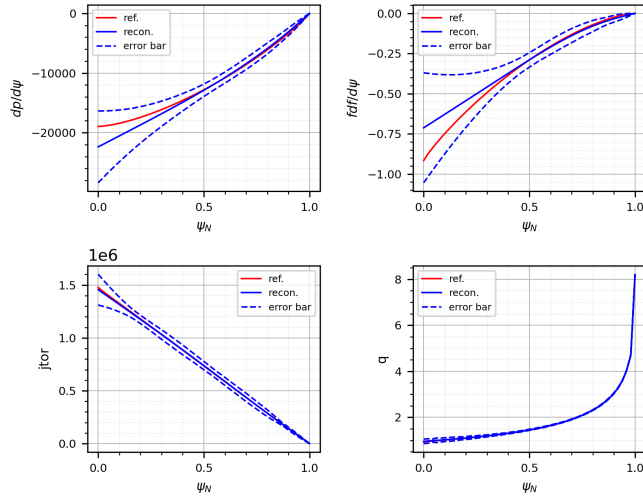


Figure 3: Top row: reference and reconstructed p' and ff' profiles as function of the normalized flux ψ_N with computed error bars. Bottom row: same for the average toroidal current density j_{tor} and safety factor q profiles.

5 Conclusion

The equilibrium code NICE is ready to use ITER data. A first equilibrium reconstruction numerical exercise using synthetic magnetic measurements has been successfully conducted. The code is fully IMAS compatible, can read and write IDS. It is also ready to use other measurements such as pressure measurements, motional Stark effect (MSE) as well as interferometry and polarimetry. The polarimetry Stokes vector modelization can also be used [13]. These internal measurements will most likely be needed to improve the accuracy of the reconstruction of the p' and ff' profiles for ITER discharges. The code NICE is already routinely used at WEST and has been tested on different tokamaks and validated against other codes within the EUROfusion program [8, 14, 29, 33, 36]. NICE is a robust code which exhibits excellent convergence properties thanks to the use of Newton and SQP methods. The code can be used for equilibrium reconstruction but also for direct static or evolutive simulations. It can also be used to solve the inverse problems consisting in finding the currents or voltages in the poloidal field coils which enable to have a desired plasma shape [9]. Finally the code NICE can be used with high order finite elements providing a smooth representation of the magnetic flux and field in the plasma [7, 32].

Acknowledgment

We would like to thank Masanari Hosokawa, Simon Pinches and Mireille Schneider for their help in providing the latest ITER machine description. We would also like to thank the anonymous reviewer for the numerous remarks and constructive criticism from which the paper has benefitted.

References

- [1] R. Albanese, J. Blum, and O. Barbieri. On the solution of the magnetic flux equation in an infinite domain. In *EPS. 8th Europhysics Conference on Computing in Plasma Physics (1986)*, pages 41–44, 1986.
- [2] J. Blum. *Numerical Simulation and Optimal Control in Plasma Physics with Applications to Tokamaks*. Series in Modern Applied Mathematics. Wiley Gauthier-Villars, Paris, 1989.
- [3] J. Blum, C. Boulbe, and B. Faugeras. Real-time plasma equilibrium reconstruction in a tokamak. In *Journal of Physics: Conference Series. Proceedings of the 6th International Conference on Inverse Problems in Engineering: Theory and Practice*, volume 135, page 012019. IOP Publishing, 2008.
- [4] J. Blum, C. Boulbe, and B. Faugeras. Reconstruction of the equilibrium of the plasma in a tokamak and identification of the current density profile in real time. *Journal of Computational Physics*, 231(3):960 – 980, 2012.
- [5] J. Blum, H Heumann, E. Nardon, and X. Song. Automating the design of tokamak experiment scenarios. *J. Computational Physics*, 394:594–614, 2019.
- [6] J. Blum, E. Lazzaro, J. O’Rourke, B. Keegan, and Y. Stefan. Problems and methods of self-consistent reconstruction of tokamak equilibrium profiles from magnetic and polarimetric measurements. *Nuclear Fusion*, 30(8):1475, 1990.
- [7] A. Elarif, B. Faugeras, and F. Rapetti. Tokamak free-boundary plasma equilibrium computation using finite elements of class C0 and C1 within a mortar element approach. *J. Computational Physics*, 439:110388, 2021. .
- [8] G. L. Falchetto, P. Strand, R. Coelho, D. Coster, J. Ferreira, T. Jonsson, D. Yadikin, R. Dumont, B. Faugeras, J. Hollocombe, P. Huynh, J. Joly, D. Kalupin, E. Lerche, J. Morales, M. Poradzinski, P. Siren, E. Tholerus, D. Van Eester, J. Varje, W. Zwingmann, JET Contributors, and EUROfusion-IM Team. Multi-machine analysis of eu experiments using the eurofusion integrated modelling (eu-im) framework. In European Physical Society, editor, *46th EPS Conference on Plasma Physics*, volume 43C of *Europhysics Conference Abstracts (ECA)*, Milan, Italy, 2019.
- [9] B. Faugeras. An overview of the numerical methods for tokamak plasma equilibrium computation implemented in the NICE code. *Fusion Eng. Design*, 160:112020, 2020.
<https://hal.archives-ouvertes.fr/hal-02955053>.
- [10] B. Faugeras, J. Blum, C. Boulbe, P. Moreau, and E. Nardon. 2D interpolation and extrapolation of discrete magnetic measurements with toroidal harmonics for equilibrium reconstruction in a Tokamak. *Plasma Phys. Control Fusion*, 56:114010, 2014.
- [11] B. Faugeras, J. Blum, H. Heumann, and C. Boulbe. Optimal control of a coupled partial and ordinary differential equations system for the assimilation of polarimetry stokes vector measurements in tokamak free-boundary equilibrium reconstruction with application to ITER. *Comput. Phys. Comm.*, 217(Supplement C):43 – 57, 2017.

- [12] B. Faugeras and H Heumann. FEM-BEM coupling methods for tokamak plasma axisymmetric free-boundary equilibrium computations in unbounded domains. *J. Computational Physics*, 343(Supplement C):201 – 216, 2017.
- [13] B. Faugeras, F. Orsitto, and JET Contributors. Equilibrium reconstruction at JET using Stokes model for polarimetry. *Nuclear Fusion*, 58(10):106032, 2018.
- [14] L. Fleury, H. Ancher, J.F. Artaud, B. Faugeras, M. Geynet, F. Hollocombe, F. Imbeaux, P. Maini, and J. Morales. WEST plasma reconstruction chain and IMAS related tools. In *SOFT 2020*, Croatia, 09 2020.
- [15] J. P. Freidberg. *Ideal Magnetohydrodynamics*. Plenum US, 1987.
- [16] G.N. Gatica and G.C. Hsiao. The uncoupling of boundary integral and finite element methods for nonlinear boundary value problems. *J. Math. Anal. Appl.*, 189(2):442–461, 1995.
- [17] Johan Peter Goedbloed and Stefaan Poedts. *Principles of magnetohydrodynamics: with applications to laboratory and astrophysical plasmas*. Cambridge university press, 2004.
- [18] H. Grad and H. Rubín. Hydromagnetic equilibria and force-free fields. *Proceedings of the 2nd UN Conf. on the Peaceful Uses of Atomic Energy*, 31:190, 1958.
- [19] Virginie Grandgirard. *Modélisation de l'équilibre d'un plasma de tokamak*. PhD thesis, Université de Franche-Comté, 1999.
- [20] H. Heumann, J. Blum, C. Boulbe, B. Faugeras, G. Selig, J.-M. Ané, S. Brémond, V. Grangirard, P. Hertout, and E. Nardon. Quasi-static free-boundary equilibrium of toroidal plasma with CEDRES++: computational methods and applications. *J. Plasma Physics*, 2015.
- [21] M. Hinze, R. Pinnau, M. Ulbrich, and S. Ulbrich. *Optimization with PDE constraints*, volume 23 of *Mathematical Modelling: Theory and Applications*. Springer, New York, 2009.
- [22] F. Imbeaux, S.D. Pinches, J.B. Lister, Y. Buravand, T. Casper, B. Duval, B. Guillerminet, M. Hosokawa, W. Houlberg, P. Huynh, S.H. Kim, G. Manduchi, M. Owsiak, B. Palak, M. Plociennik, G. Rouault, O. Sauter, and P. Strand. Design and first applications of the ITER integrated modelling & analysis suite. *Nuclear Fusion*, 55(12):123006, 2015.
- [23] S.C. Jardin. *Computational methods in plasma physics*. Boca Raton, FL : CRC Press/Taylor & Francis, 2010.
- [24] L.L. Lao. Separation of β_p and l_i in tokamaks of non-circular cross-section. *Nuclear Fusion*, 25(11):1421, 1985.
- [25] L.L. Lao, J.R. Ferron, R.J. Geobner, W. Howl, H.E. St. John, E.J. Strait, and T.S. Taylor. Equilibrium analysis of current profiles in Tokamaks. *Nuclear Fusion*, 30(6):1035, 1990.
- [26] R. Lüst and A. Schlüter. Axialsymmetrische magnetohydrodynamische Gleichgewichtskonfigurationen. *Z. Naturforsch. A*, 12:850–854, 1957.
- [27] J.L. Luxon and B.B. Brown. Magnetic analysis of non-circular cross-section tokamaks. *Nuclear Fusion*, 22(6):813–821, 1982.
- [28] P.J. Mc Carthy, P. Martin, and W. Schneider. The CLISTE Interpretive Equilibrium Code. Technical Report IPP Report 5/85, Max-Planck-Institut für Plasmaphysik, 1999.
- [29] A. Merle, R. Coelho, F. Carpanese, S. Dixon, M. Dunne, B. Faugeras, L. Fleury, J. Hollocombe, F. Imbeaux, L. Kogan, M. Romanelli, O. Sauter, W. Zwingmann, ASDEX-Upgrade team, JET contributors, MAST team, TCV team, and EUROfusion-IM team. Equilibrium reconstruction of discharges from eurofusion tokamaks using the wpcd scientific workflows. In *European Physical*

Society, editor, *47th EPS Conference on Plasma Physics*, volume 45A of *Europhysics Conference Abstracts (ECA)*, page P2.1036, Milan, Italy, June 2021.

- [30] J.-M. Moret, B.P. Duval, H.B. Le, S. Coda, F. Felici, and H. Reimerdes. Tokamak equilibrium reconstruction code LIUQE and its real time implementation. *Fusion Eng. Design*, 91(0):1–15, 2015.
- [31] J. Nocedal and S. J. Wright. *Numerical optimization*. Springer Series in Operations Research and Financial Engineering. Springer, New York, second edition, 2006.
- [32] F. Rapetti, B. Faugeras, and C. Boulbe. High-order finite elements in tokamak free-boundary plasma equilibrium computations. In *ICOSAHOM 2020(2021) International Conference on Spectral and High Order Methods*, Vienna, Austria, July 2021.
- [33] R. Santos, R. Coelho, P. Rodrigues, B. Faugeras, H. Fernandes, B. B. Carvalho, D. Corona, H. Figueiredo, and H. Alves. Plasma boundary reconstruction in ISTTOK using magnetic diagnostic data. *Journal of Instrumentation*, 14(09):C09019–C09019, 2019.
- [34] V D Shafranov. Determination of the parameters β_p and l_i in a tokamak for arbitrary shape of plasma pinch cross-section. *Plasma Physics*, 13(9):757, 1971.
- [35] V.D. Shafranov. On magnetohydrodynamical equilibrium configurations. *Soviet Journal of Experimental and Theoretical Physics*, 6:545, 1958.
- [36] X. Song, X.M. Song, B. Li, J. Zhou, E. Nardon, H. Heumann, B. Faugeras, J.X. Li, Sh Wang, SH.Y. Liang, J.Z. Zhang, T.F Sun, W.B Li, Zh.H. Huang, L. Liu, Z.C. Yang, H.X. Wang, X.Q. Ji, W.L. Zhong, and HL-2M Team. Plasma initiation and preliminary magnetic control in the HL-2M tokamak. *Nuclear Fusion*, 61(8):086010, 2021. <https://doi.org/10.1088/1741-4326/ac09fc>.
- [37] D.W. Swain and G.H. Neilson. An efficient technique for magnetic analysis for non-circular, high-beta tokamak equilibria. *Nuclear Fusion*, 22(8):1015–1030, 1982.
- [38] J. Wesson. *Tokamaks*. The International Series of Monographs in Physics. Oxford University Press, 2004.
- [39] L.E. Zakharov and V.D. Shafranov. Equilibrium of a toroidal plasma with noncircular cross-section. *Sov. Phys. Tech. Phys.*, 18(2):151–156, 1973.
- [40] W. Zwingmann. Equilibrium analysis of steady state tokamak discharges. *Nuclear Fusion*, 43:842–850, 2003.